

Supporting Information

Co-supported on N-doped carbon, derived from bimetallic azolate
framework-6: Highly effective oxidative desulfurization catalyst

Biswa Nath Bhadra, Nazmul Abedin Khan, and Sung Hwa Jung*

Department of Chemistry and Green-Nano Materials Research Center, Kyungpook National
University, Daegu 41566, Republic of Korea

*Corresponding author: Prof. Sung Hwa Jung

Phone: +82-10-2818-5341; Fax: +82-53-950-6330

E-mail: sung@knu.ac.kr

1. Experimental methods

1.1. Synthesis and pyrolysis of bimetallic MAF-6s

Synthesis of bimetallic MAF-6s. To Synthesize MAF-6(100Zn) and MAF-6(x Zn y Co), at first, a required amount (based on the composition) of Zn(OH)₂ was dissolved in aqueous ammonia solution (25%) and a suitable amount of cobalt acetate was added to the solution. Then, 2-ethylimidazole was dissolved in a premixed solvent of ethanol and cyclohexane. For the MAF-6(100Co) synthesis, cobalt acetate dehydrate was dissolved in ethanol (100 mL) and 2-ethylimidazole was dissolved in separate beaker having a premixed solvent of ethanol (100 mL), cyclohexane (50 mL) a TEA (8.0 g). The amount of applied reagents for MAF-6s are shown in Table S1. The first solution was added rapidly to the second solution under stirring, and the mixture was stirred for 15 min at room temperature (~ 25 °C). The precipitate was collected by filtration and washed with ethanol. The obtained product was dried at 100 °C in an oven for the next use.

Pyrolysis of bimetallic MAF-6s. The pyrolysis of the obtained bimetallic MAF-6s was conducted at a set temperature (800, 900 and 1000 °C) for 2 h under continuous N₂ (50 mL/min) flow using a tube furnace. An alumina boat containing 1.0 g of MAF-6(x Zn y Co) was placed in the furnace and the temperature was increased from room temperature to the desired temperature with a ramping rate of 2 °C/min. After pyrolysis for 2 h under the set temperature, the boat was cooled to room temperature with a cooling rate of 2 °C/min and the materials were collected. The MDC-6(x Zn y Co)-Ts were then leached with 0.5 M H₂SO₄ for 24 h at 60 °C to remove any soluble species.

1.2. Synthesis of Co/AC and Co/rGO

AC was collected from the commercially available source (Duksan Pure Chemical Co. Ltd.). However, rGO was prepared by two-step methods including the oxidation of graphite powder by using NaNO₃, concentrated H₂SO₄ and KMnO₄¹ and reduction by using NaBH₄,² similar to the

reported methods. A fixed amount of AC or rGO was added to a cobalt acetate solution in ethanol and the suspension was stirred for overnight, and the solution was evaporated using a rotary evaporator under vacuum at 50 °C to get a solid product. The obtained solid was then annealed in a tube-furnace at 750 °C for 6 h under N₂ flow to give the Co/AC and Co/rGO.³

1.3. Characterization

The crystal phases of the prepared materials were examined by the corresponding powder X-ray diffraction. The size of the particles was estimated from the XRD peaks using the Scherrer equation. The unit cell parameters were estimated from eight most intense peaks (precise diffraction positions were got using α -Al₂O₃ as an external standard) of MAF-6s with a standard least squares refinement technique by WINCELL 1.1. The N₂ adsorption-desorption isotherms were measured at -196 °C after the evacuation of the samples at 150 °C for 6 h. The surface areas and pore size distributions were evaluated using the Brunauer–Emmett–Teller (BET) (at a relative pressure of 0.05–0.20) and Barrett–Joyner–Halenda (BJH) (from the desorption branches) methods, respectively. The crystal morphologies, particle size, distribution of particles, and lattice fringe spacing of the selected materials were investigated using an FE-TEM. Raman spectra were recorded at room temperature using a UV micro Raman spectrometer having a Leica DMLM microscope in the range 200–3000 cm⁻¹. X-ray photoelectron spectroscopy (XPS), a Quantera SXM spectrometer (ULVAC-PHI) assembled with a dual beam charge neutralizer, was used to analyze surface properties of MDC-6(75Zn25Co)-900. The chemical compositions (Co and Zn) were evaluated by FE-TEM EDS or inductively coupled plasma (ICP)-optical emission spectrometry.

1.4. Evaluation of catalytic activities

Oxidation of DBT. To the DBT solution (20 mL, 1,000 mg/L, in n-octane) in a glass reactor (50 mL) equipped with a condenser, acetonitrile (5 mL), H₂O₂ (0.2 mL, 30% aqueous solution; oxidant to sulfur molar ratio (O/S) = 15) was heated up to 70 °C and dried catalyst (10 mg) were added. Then the reaction mixtures were vigorously stirred for set time. Acetonitrile was used as an extractive solvent, H₂O₂ acted as an oxidant; and, MDC-6(75Zn25Co)-900, Co/AC and Co/rGO were applied as the catalysts. The liquid portion was separated by filtration after the reaction mixture was cooled down to room temperature. The n-octane (nonpolar) and acetonitrile (polar) phases were separated, and the residual concentration of DBT in the n-octane was analyzed using UV absorbance at 325.6 nm (with UV-1800, Shimadzu). The product extracted from the CH₃CN phase was analyzed using a GC-MS (Agilent, 7890A-5975C GC/MSD). Using a very similar reaction composition/method, the oxidations of thiophene, benzothiophen, and 4,6-dimethyldibenzothiophene were conducted at 70 °C for 120 min.

At first, the effect of mixing speed (rpm) on the oxidation of DBT using the MDC-6(75Zn25Co)-900 was checked by conducting the reactions with stirring speed ranged from 100 to 1000 rpm for 120 min at 70 °C. After fixing 500 rpm as the optimum stirring speed, oxidation of DBT was also conducted with Co/AC and Co/rGO as catalysts. Oxidation of DBT was conducted at two other temperatures (e.g. 30 and 50 °C) with MDC-6(75Zn25Co)-900 and Co/rGO not only to investigate the reaction kinetics at different temperatures but also to determine the activation energy of the catalysis.

Batch adsorption of DBT was conducted at 70 °C using MDC-6(75Zn25Co)-900 to understand the contribution of adsorption on the removal of DBT from the model fuel. The adsorption experiments were done similar to the oxidative desulfurization (ODS) only in the absence of H₂O₂.

The mixture, maintained at 70 °C, was shaken for set time. The liquid portion was collected by filtration and residual DBT in n-octane was analyzed similarly using UV absorbance.

Reduction of 4-NP. The MDC-6(75Zn25Co)-900, Co/AC and Co/rGO were applied as catalysts in the reduction of 4-NP in water. For the catalytic reduction of 4-NP, aqueous solution of 4-NP (20 mL, 1000 mg/L) was mixed with the freshly prepared NaBH₄ aqueous solution (0.5 M, 1.0 mL). Then the catalyst (0.01 g) was added to the reaction mixture, and the reaction was monitored by UV absorbance at 400 nm, similar to a reported procedure.^{4,5}

Recycling of catalysts. The recyclability of the catalysts MDC-6(75Zn25Co)-900 was examined for the oxidation of DBT after adequate regeneration. The catalyst was separated by filtration from the reaction mixture after each catalytic reaction. The separated MDC-6(75Zn25Co)-900 was washed thoroughly with ethanol, and then dried under vacuum at 100 °C for overnight for the next uses.

Table S1 Composition of chemicals for the synthesis of MAF-6s.

Chemicals	MAF-6 (100Zn)	MAF-6 (75Zn25Co)	MAF-6 (50Zn50Co)	MAF-6 (25Zn75Co)	MAF-6 (100Co) ^a
Zn(OH) ₂ (g)	2.0	1.5	1.0	0.5	0
Co(OAC) ₂ (g)	0	1.2	2.5	3.7	2.5
NH ₃ (25%) (mL)	400	300	200	100	TEA = 8.0 g
EtOH (mL)	280	280	280	280	200
Cyclohexane (mL)	20	20	20	20	50
2-ethylimidazole (g)	3.85	3.85	3.85	3.85	7.6

^aTEA = triethylamine

Table S2 Textural properties of MAF-6s.

Materials	SA _{BET} (m ² ·g ⁻¹)	PV _{total} (cm ³ ·g ⁻¹)	PV _{micro} (cm ³ ·g ⁻¹)
MAF-6(100Zn)	1317	0.71	0.47
MAF-6(75Zn25Co)	1360	0.69	0.51
MAF-6(50Zn50Co)	1295	0.74	0.44
MAF-6(25Zn75Co)	1264	0.65	0.47
MAF-6(100Co)	1187	0.70	0.47

Table S3 Unit cell parameters of MAF-6s.

Materials	a=b=c (Å)	Cell volume (Å ³)
MAF-6(100Zn)	29.26	25046.26
MAF-6(75Zn25Co)	29.22	24948.28
MAF-6(50Zn50Co)	29.19	24871.52
MAF-6(25Zn75Co)	29.14	24743.92
MAF-6(100Co)	29.11	24667.58

Table S4 Compositions of BMMAF-6s analyzed by TEM-EDS/ICP.

Materials	C (wt%)	N (wt%)	Zn (wt%)	Co (wt%)	(Co×100)/(Zn+Co) ^{a,*}
MAF-6(25Zn75Co)	70.4	12.4	5.4 (5.4)*	11.5 (11.4)*	70 (70)*
MAF-6(50Zn50Co)	69.8	13.1	9.3 (9.4)*	7.4 (7.4)*	47 (47)*
MAF-6(75Zn25Co)	73.8	12.7	10.8 (10.6)*	2.1 (2.0)*	18 (17)*

^a: The relative atom % of Co was estimated by using the equation , $100 \times \text{Co}/(\text{Zn}+\text{Co})$, after converting the wt% of Co and Zn into atom%.

* Analyzed with ICP.

Table S5 Activation energies of various catalysts for oxidative desulfurization of DBT using H₂O₂ as an oxidant.

Catalysts	E_a (KJ·mol ⁻¹)	Ref.
WO ₃ /TiO ₂	54	6
NaPW	30.9	
SiW	28.3	7
PMo	29.0	
PMo/BzPN-SiO ₂	47	8
HPW-PDMAEMA-SiO ₂	23	9
HPW-IL/SBA-15	56.6	10
H-TiNT	46.2	11
TiO ₂ -SiO ₂	43.8	12
VO ₂ (rutile)	30	13
TiO ₂ @M-6	23.3	14
Co/rGO	38	This work
MDC-6(75Zn25Co)-900	25	This work

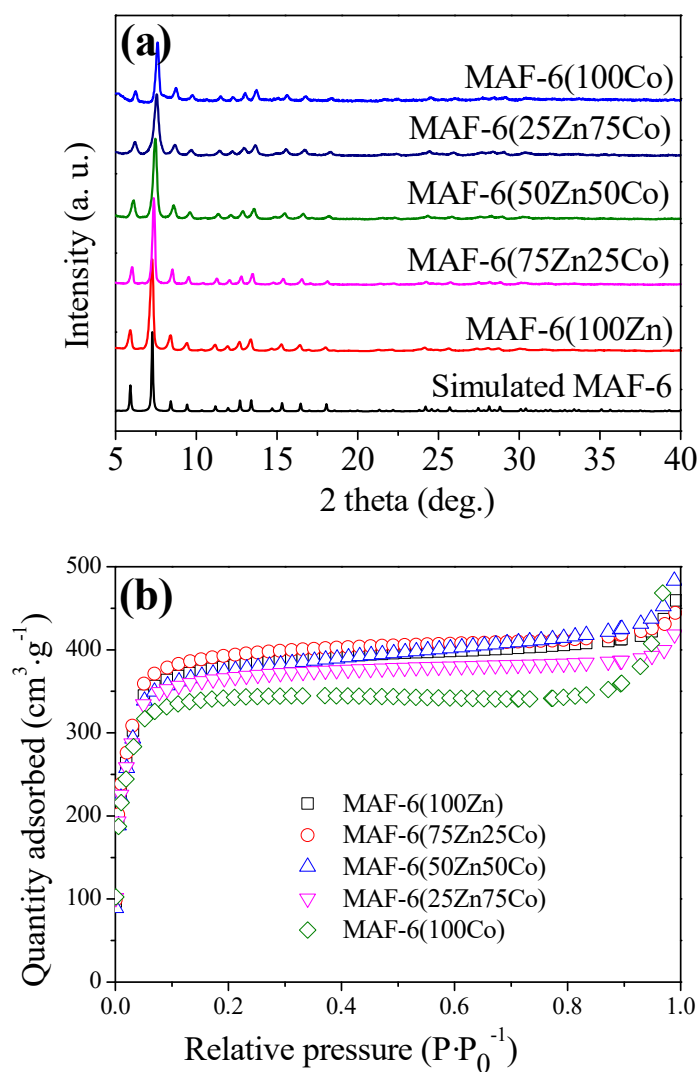


Figure S1 XRD patterns and (b) N₂ adsorption isotherms of the synthesized MAF-6(100Zn), MAF-6(75Zn25Co), MAF-6(50Zn50Co), MAF-6(25Zn75Co) and MAF-6(100Co). Simulated XRD pattern of the MAF-6 is also shown on figure a, for comparison.

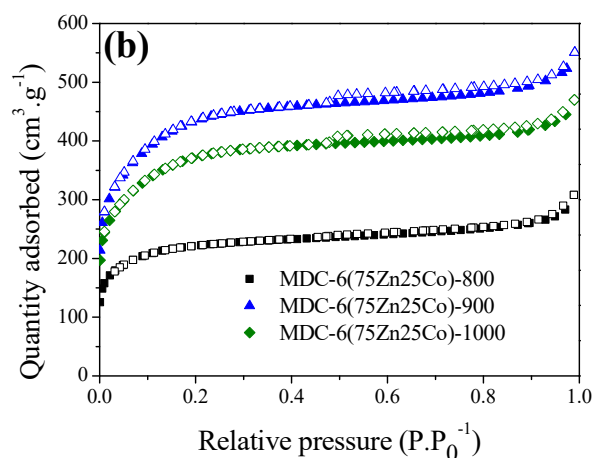
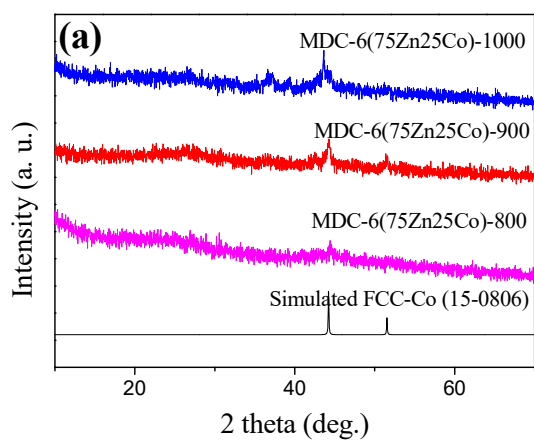


Figure S2 XRD patterns and (b) N₂ adsorption/desorption isotherms of the products obtained after carbonization of the MAF-6(75Zn25Co) at 800, 900 and 1000 °C for 2 h under N₂ flow. Simulated XRD patterns of the FCC Co is also shown on figure a, for comparison.

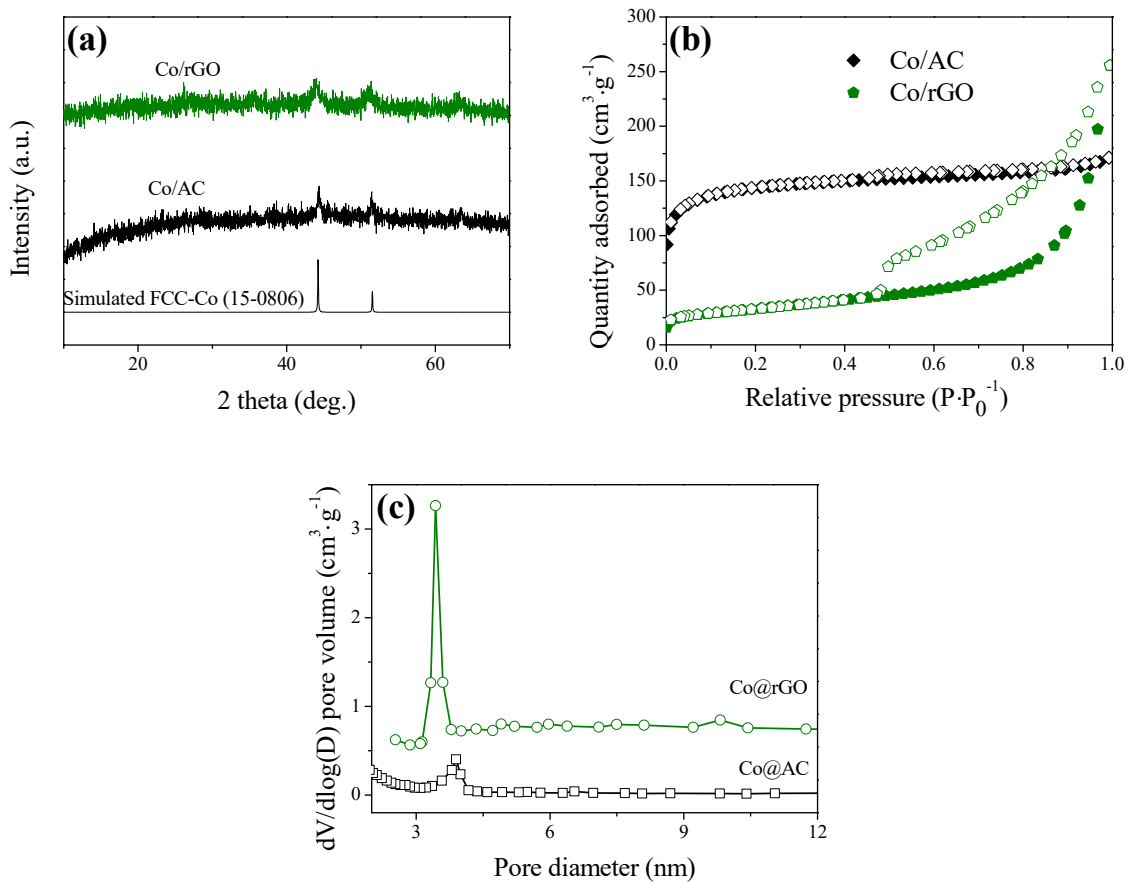


Figure S3 (a) XRD pattern, (b) N₂ adsorption/desorption isotherms and (c) pore size distribution curves of Co/AC and Co/rGO. The PSD curves were generated from the desorption branches of N₂ adsorption/desorption isotherms. Simulated XRD pattern of the FCC Co is also shown on figure a, for comparison.

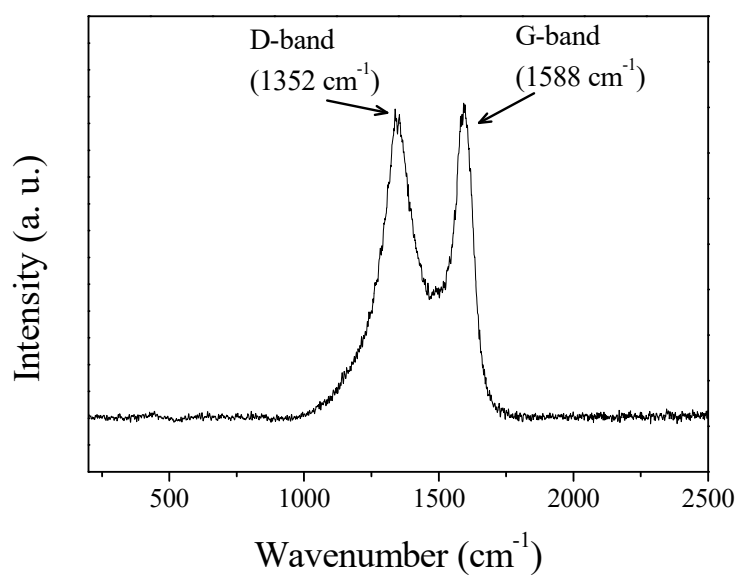


Figure S4 Raman spectrum of MDC-6(75Zn25Co)-900.

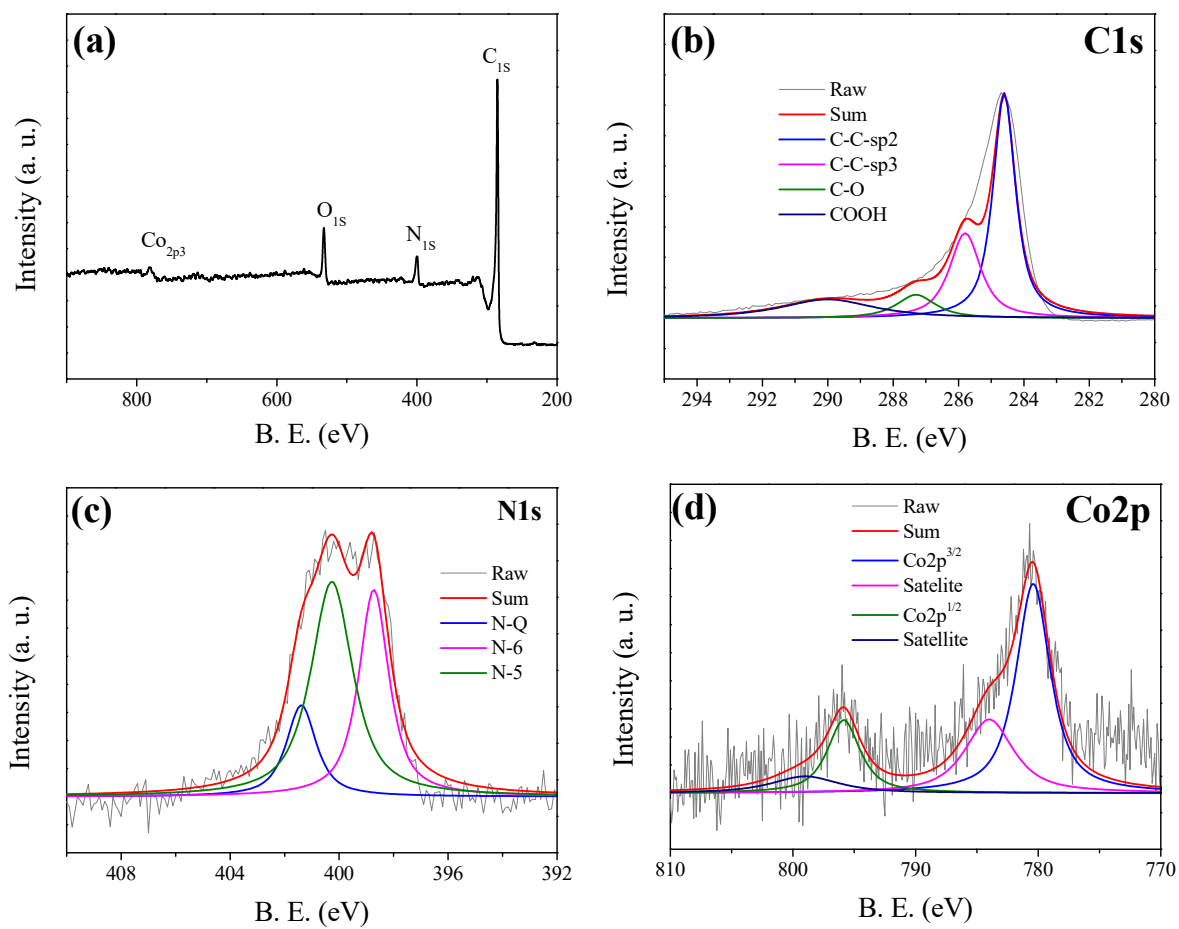


Figure S5 (a) XPS survey spectrum, and high resolution (b) C_{1s} , (c) N_{1s} and (d) Co_{2p} spectra of MDC-6(75Zn25Co)-900.

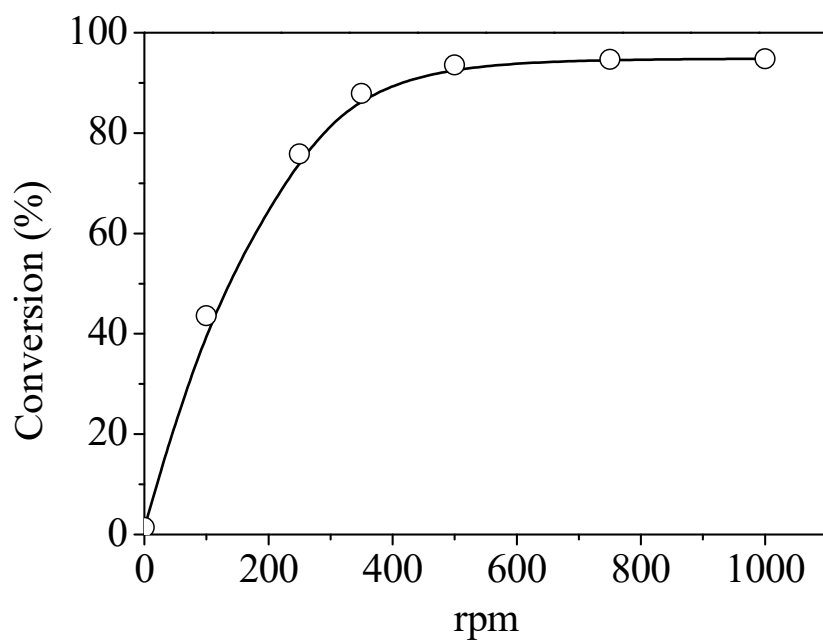


Figure S6 Effect of mixing speed (rpm) on the conversion of DBT over the MDC-6(75Zn25Co)-900 catalyst. The reaction was carried out at 70 °C for 2 h with 0.01 g of catalyst in 20 mL of a model fuel solution (DBT: 1,000 mg/L).

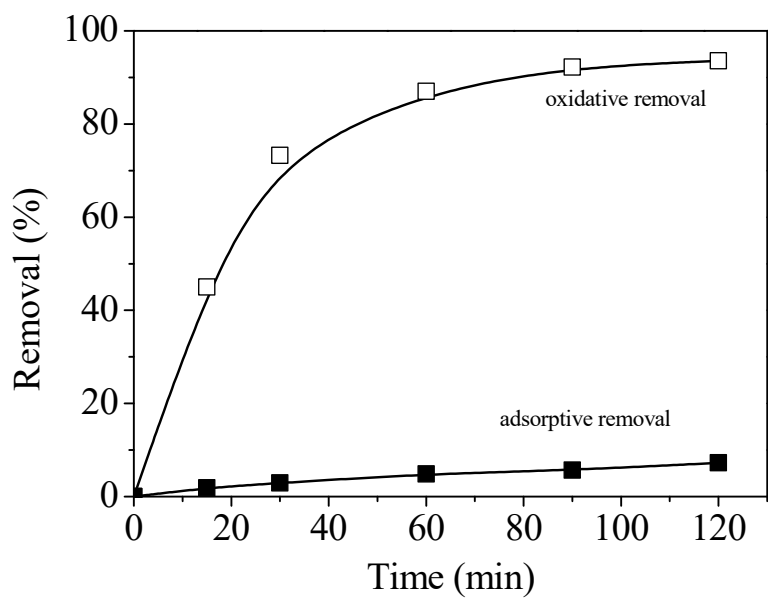


Figure S7 Effect of time on removal of DBT *via* oxidation/adsorption (empty symbols) and adsorption (filled symbols) over MDC-6(75Zn25Co)-900 at 70 °C.

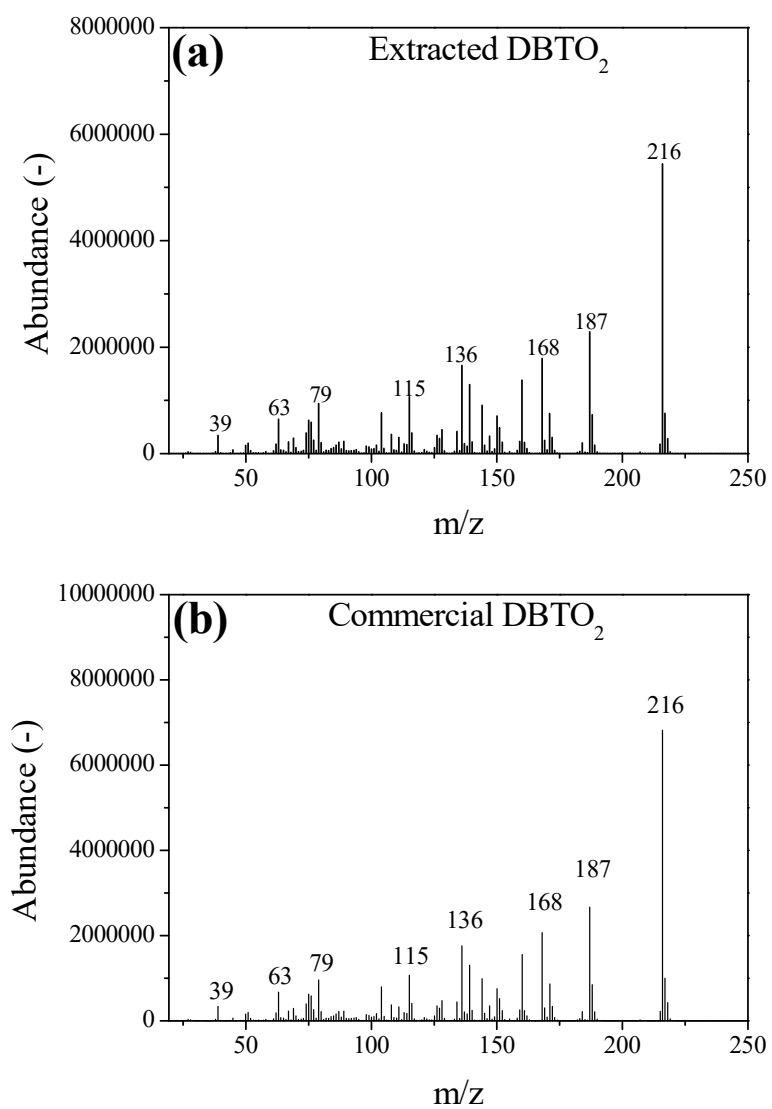


Figure S8 Fragmentation pattern of the mass spectra for the (a) product extracted in the ODS of DBT and (b) commercial DBTO₂.

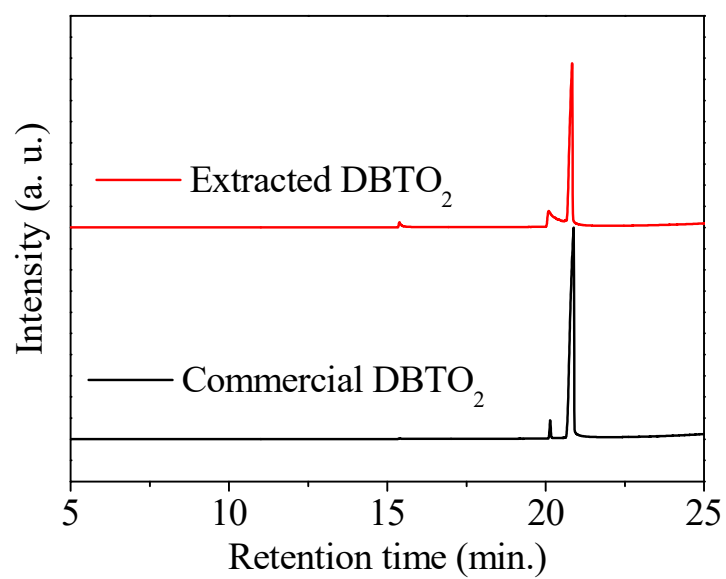


Figure S9 GC spectra of commercial DBTO₂ and DBTO₂ produced *via* catalytic oxidation of DBT. Produced DBTO₂ was extracted from the polar phase (CH₃CN) of the reaction mixture.

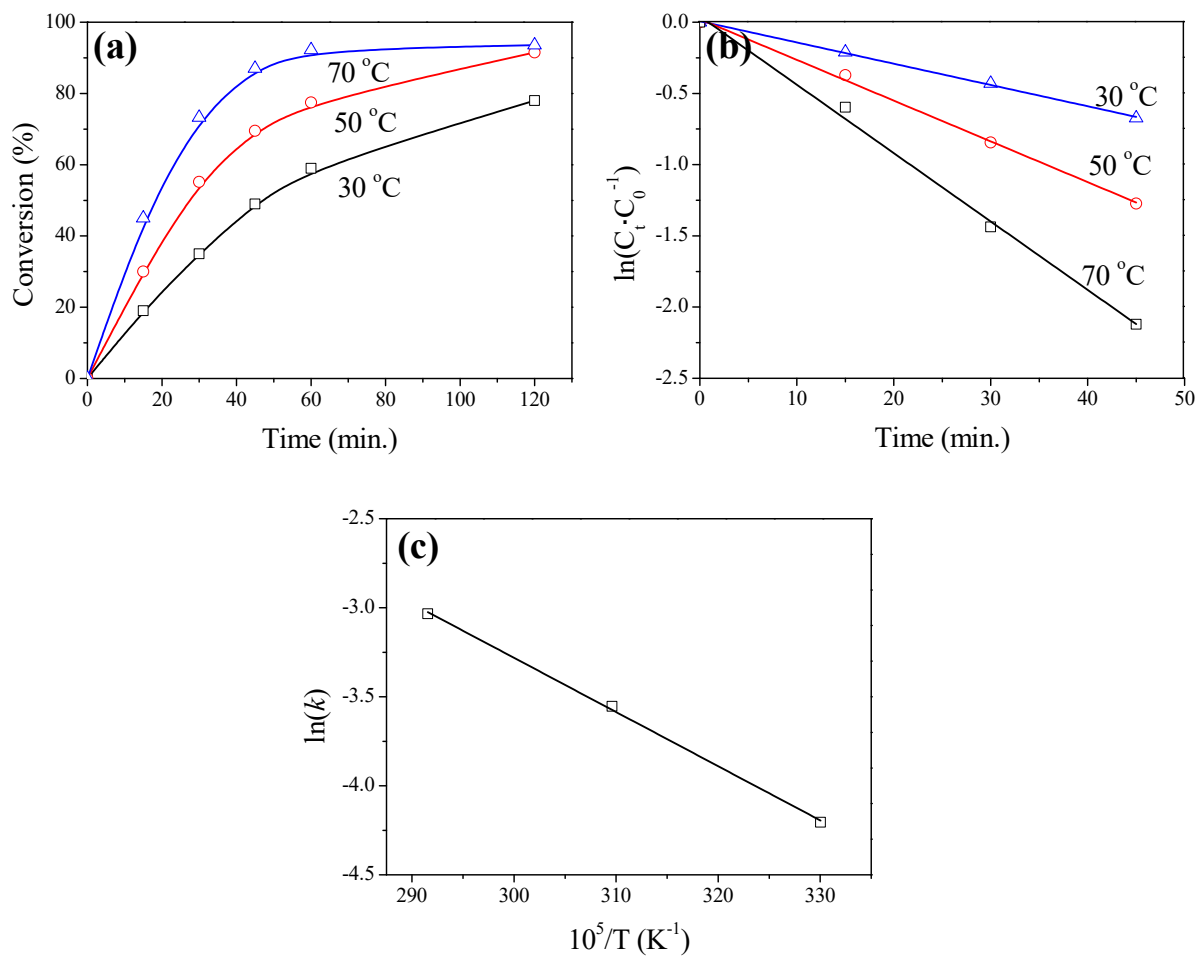


Figure S10 (a) Effect of reaction time on the DBT conversion, (b) plots of the pseudo-first-order kinetics plots and (c) Arrhenius plot to get the activation energy for the oxidation of DBT with the catalyst MDC-6(75Zn25Co)-900. Reaction temperatures are shown on figures a and b.

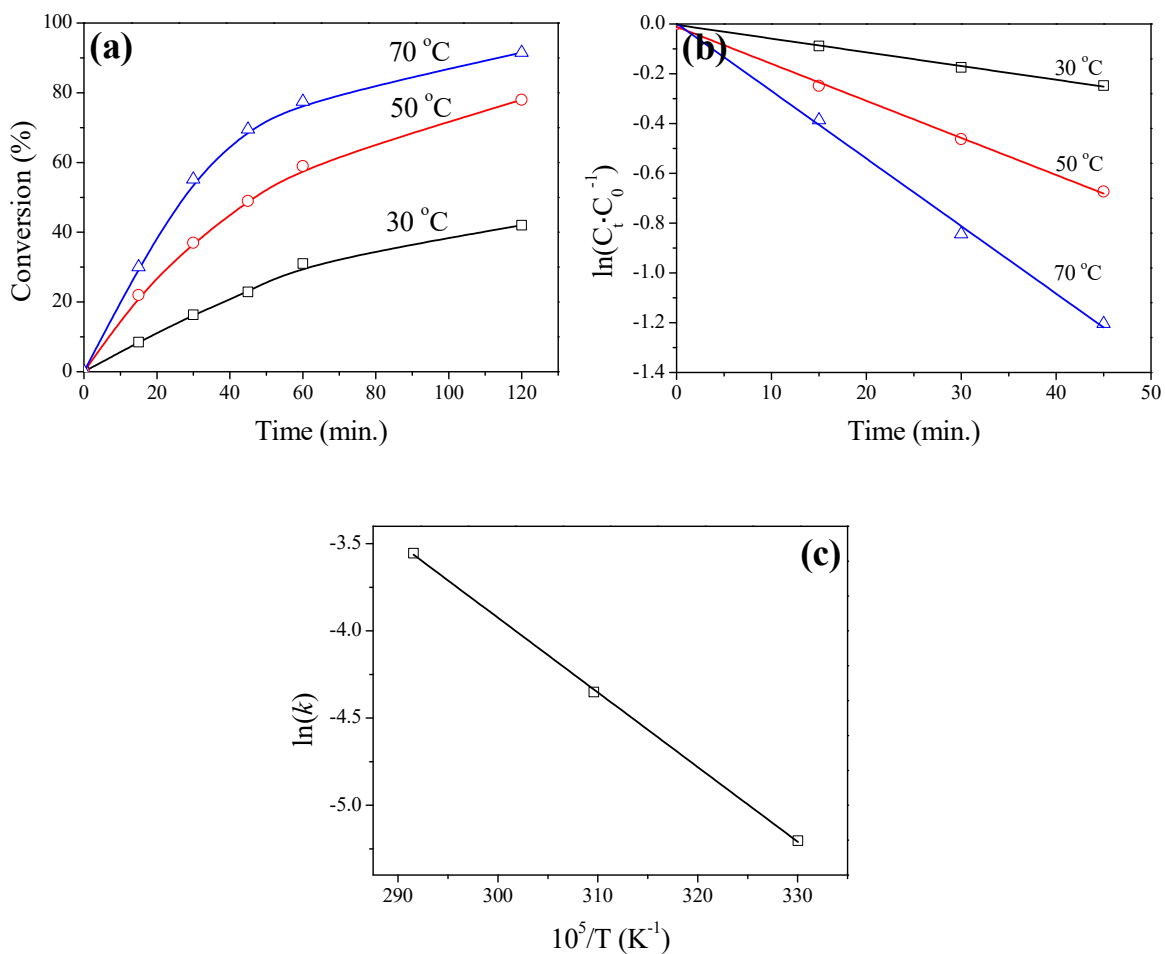


Figure S11 (a) Effect of time, (b) plots of the pseudo-first-order kinetics plots and (c) Arrhenius plot to get the activation energy for the oxidation of DBT with the catalyst Co/rGO.

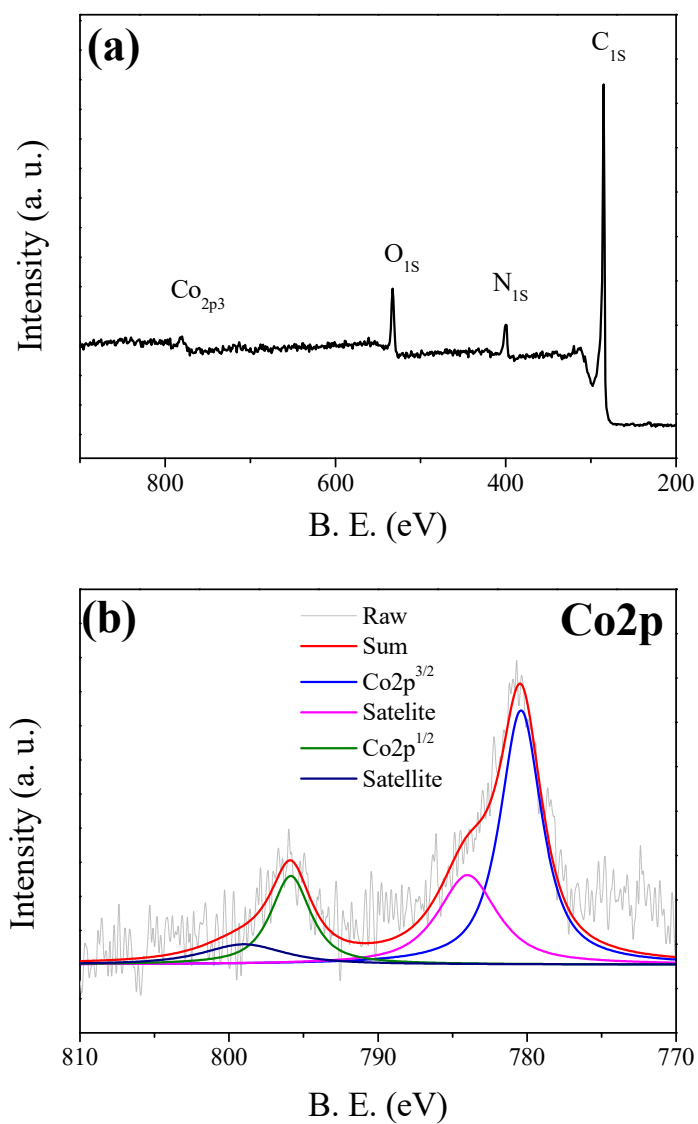


Figure S12 (a) XPS survey spectrum, and high resolution (b) Co_{2p} spectra of the recycled MDC-6(75Zn25Co)-900.

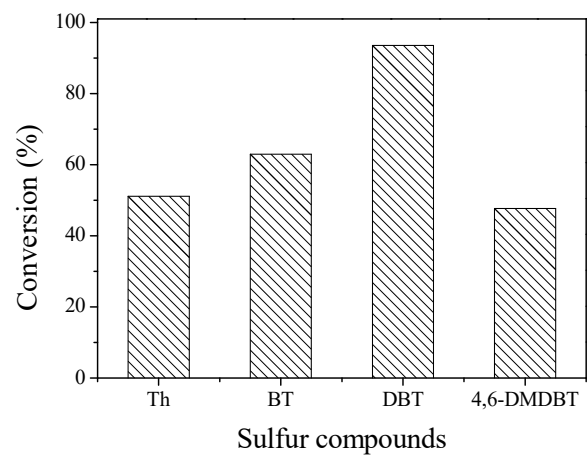


Figure S13 Conversion of Th, BT, DBT and DMDBT over MDC-6(75Zn25Co)-900 at 70 °C for 120 min.

References

1. I. Ahmed, N. A. Khan and S. H. Jung, *Inorg. Chem.*, 2013, **52**, 14155-14161.
2. A. Ambrosi, C. K. Chua, A. Bonanni and M. Pumera, *Chem. Mater.*, 2012, **24**, 2292-2298.
3. P. R. Shukla, S. Wang, H. Sun, H. M. Ang and M. Tadé, *Appl. Catal., B*, 2010, **100**, 529-534.
4. B. N. Bhadra and S. H. Jung, *Nanoscale*, 2018, **10**, 15035-15047.
5. Z. Hasan, D.-W. Cho, C.-M. Chon, K. Yoon and H. Song, *Chem. Eng. J.*, 2016, **298**, 183-190.
6. Y. Qin, S. Xun, L. Zhan, Q. Lu, M. He, W. Jiang, H. Li, M. Zhang, W. Zhu and H. Li, *New J. Chem.*, 2017, **41**, 569-578.
7. A. E. S. Choi, S. Roces, N. Dugos and M.-W. Wan, *Fuel*, 2016, **180**, 127-136.
8. M. Craven, D. Xiao, C. Kunstmann-Olsen, E. F. Kozhevnikova, F. Blanc, A. Steiner and I. V. Kozhevnikov, *Appl. Catal., B*, 2018, **231**, 82-91.
9. M. Zhu, G. Luo, L. Kang and B. Dai, *RSC Adv.*, 2014, **4**, 16769-16776.
10. J. Xiong, W. Zhu, W. Ding, L. Yang, Y. Chao, H. Li, F. Zhu and H. Li, *Ind. Eng. Chem. Res.*, 2014, **53**, 19895-19904.
11. E. Lorençon, D. C. B. Alves, K. Krambrock, E. S. Ávila, R. R. Resende, A. S. Ferlauto and R. M. Lago, *Fuel*, 2014, **132**, 53-61.
12. A. Bazyari, A. A. Khodadadi, A. H. Mamaghani, J. Beheshtian, L. T. Thompson and Y. Mortazavi, *Appl. Catal., B*, 2016, **180**, 65-77.
13. K. Chen, N. Liu, M. Zhang and D. Wang, *Appl. Catal., B*, 2017, **212**, 32-40.
14. M. Sarker, B. N. Bhadra, S. Shin and S. H. Jung, *ACS Appl. Nano Mater.*, 2019, **2**, 191-201.